



Published in final edited form as:

Osteoarthritis Cartilage. 2021 June ; 29(6): 915–923. doi:10.1016/j.joca.2021.02.565.

Immune Cell Profiling in the Joint following Human and Murine Articular Fracture

Bridgette D. Furman¹, Jacob Zeitlin¹, Michael W. Buchanan¹, Janet L. Huebner², Virginia B. Kraus^{2,3}, John S. Yi⁴, Samuel B. Adams¹, Steven A. Olson¹

¹Department of Orthopaedic Surgery, Duke University Medical Center, Durham, NC 27710

²Duke Molecular Physiology Institute, Durham, NC 27701

³Department of Medicine, Duke University School of Medicine, Durham, NC 27710

⁴Department of Surgery, Duke University Medical Center, Durham, NC 27710

Abstract

Objective: Human and *in vivo* animal research implicates inflammation following articular fracture as contributing to post-traumatic arthritis. However, relevant immune cell subsets present following injury are currently undefined. Immunophenotyping human and murine synovial fluid may help to identify immune cell populations that play key roles in the response to articular fracture.

Methods: Immunophenotyping by polychromatic flow cytometry was performed on human and mouse synovial fluid following articular fracture. Specimens were collected in patients with closed ankle fracture at the time of surgical fixation and from C57BL/6 mice with closed articular knee fracture. Immune cells were collected from injured and uninjured joints in mice via a novel cell isolation method. Whole blood samples were also collected. Immunohistochemistry (IHC) was performed on mouse synovial tissue to assess for macrophages and T cells.

Results: Following intra-articular fracture, the prominent human synovial fluid immune cell subset was CD3+ T cells, containing both CD4+ and CD8+ T cells. In mice, infiltration of CD45+ immune cells in synovial fluid of the fractured limb was dominated by CD19+ B cells and CD3+ T cells at 7 days after intra-articular fracture. We also detected adaptive immune cells, including macrophages, NK cells, dendritic cells and monocytes. Macrophage and T cell findings were supported by IHC of murine synovial tissue.

Corresponding author: Steven A. Olson, M.D. Duke University Medical Center, Box 3389, Durham, NC 27710, Tel (919) 668-3000, Fax (919) 668-2933, olson016@dm.duke.edu.

Author Contributions: Study conception and design: SAO, SBA, JSY. Acquisition of data: BDF, JZ, MWB, JLH, JSY. Data analysis and interpretation: BDF, JZ, MWB, JLH, VBK, JSY, SBA, SAO. Drafting of manuscript: BDF, JZ, MWB, JSY, SBA, SAO. Manuscript preparation: BDF, JZ, MWB, JSY, SBA, SAO, JLH, VBK. All authors revised the manuscript critically for important intellectual content and approved the final submitted manuscript.

Conflicts of Interest: The authors have no financial or personal relationships that could potentially influence or bias this work and conclusions.

Publisher's Disclaimer: This is a PDF file of an unedited manuscript that has been accepted for publication. As a service to our customers we are providing this early version of the manuscript. The manuscript will undergo copyediting, typesetting, and review of the resulting proof before it is published in its final form. Please note that during the production process errors may be discovered which could affect the content, and all legal disclaimers that apply to the journal pertain.

Conclusions: Determining specific cell populations that mediate the immune response is essential to elucidating the chain of events initiated after injury and may be an important step in identifying potential immune signatures predictive of PTA susceptibility or potential therapeutic targets.

Keywords

trauma; injury; intra-articular fracture; immunophenotype; post-traumatic arthritis

Introduction:

Traumatic injuries of articular joints are common and can lead to the progression of post-traumatic arthritis (PTA) [1]. A spectrum of articular injuries have the potential to develop into PTA, including soft tissue strains and tears, ligament partial tears and rupture, and articular fractures [1–3]. Articular fractures, which often occur in younger patients, are particularly problematic in that even with current treatment of surgical restoration of the articular surface PTA can develop within a year of injury resulting in joint dysfunction, pain, and long-term disability [1, 4–6]. There are no mitigating therapies for PTA in these injuries. Unfortunately, the mechanism of PTA development following articular fracture is not fully elucidated.

Inflammation is recognized both as a normal aspect of the biologic response to articular injury and as a pathologic mechanism linked to the development of arthritis. Acutely following trauma to articular joints, pro-inflammatory cytokines and chemokines are elevated in synovial fluid and synovium [7–10]. Recently, modulation of this inflammatory response has been explored as a therapeutic strategy to mitigate the severity of PTA. *In vivo* work demonstrated that early intra-articular inhibition of IL-1 signaling using IL-1 receptor antagonist (IL-1Ra) prevented the development of PTA in a murine closed articular fracture model [11–13]. Clinically, use of IL-1Ra (anakinra) for treatment of rheumatoid arthritis (RA) has demonstrated both decreased cellular migration and altered T cell differentiation in the synovium [14–16], and inhibition of IL-1 in a mouse model of systemic sclerosis altered T cell and macrophage phenotypes [17]. Elevated pro-inflammatory cytokines are found in synovial fluid of human patients within 24 hours after an articular fracture [7, 10]. However, the immune cells contributing to early inflammation and the development of PTA have not been characterized in human or murine models. It may be important to identify which cell subsets are involved to develop potential therapeutic targets and identify immune signatures that are predictive of PTA susceptibility. Techniques to identify immune cells following articular fractures can be problematic, as bleeding into the joint space, or hemarthrosis, can lead to technical challenges in isolating immune cells. Identifying the cellular subsets of immune cells after acute articular fracture is crucial to understanding the biological consequences of fracture, but immunophenotyping of synovial fluid cells following articular fracture has not been reported.

The objective of this study was to assess the feasibility of human and mouse synovial fluid immunophenotyping via polychromatic flow cytometry following intra-articular fracture to define both innate and adaptive immune cell populations that may play key roles in the

response to articular fracture and PTA development. For this purpose, we implemented novel cell isolation methods from synovial fluid in the human ankle and mouse knee following articular fracture. With additional histologic assessment of immune cells in mouse synovial tissue, we compared human and murine immune signatures after fracture. We hypothesized that similar phenotypes of immune cells are present in human and murine synovial fluid following intra-articular fracture.

Materials and Methods:

Human Articular Fracture Synovial Fluid.

Under an IRB-approved protocol, synovial fluid was obtained from 6 patients (mean age 40; ranging from 18–65 years of age) with closed intra-articular ankle fractures (Figure 1A). All aspirations were performed at the time of surgery after tourniquet inflation. We utilized a variation of a technique described by Adams et al. to measure cytokines in synovial fluid after intra-articular fracture [8]. Using a standard anteromedial arthroscopy portal approach, a 16-gauge needle attached to a 10cc syringe was inserted into the joint under fluoroscopic guidance. The contents of the joint were aspirated and transferred to Eppendorf tubes.

The synovial fluid samples were then centrifuged at room temperature for 15 mins at a speed of 3500 rpm to remove particulate matter, followed by a red blood cell lysis using BD PharmLyse, an ammonium chloride based lysing buffer (BD; San Jose, CA). The supernatant was removed and stored at -80°C for future analyses [18]. The cells isolated from the cell pellet were transferred to a 96 well round-bottom plate and stained using a panel of fluorescent antibodies [19]. Briefly, synovial-fluid derived cells were first incubated with a viability dye to detect dying cells followed by a surface stain with an antibody cocktail that includes markers for innate and adaptive cell subsets (Figure 1B). The unbound antibodies were washed out by centrifugation and stained cells were fixed with 1% paraformaldehyde prior to acquisition on a BD LSRII flow cytometer (BD; San Jose, CA).

Mouse Articular Fracture Model.

An established mouse model of articular fracture of the knee was used to assess the immune cell response in a preclinical model (Figure 2A). All procedures were performed under an IACUC approved protocol. Twenty-two adult male C57BL/6 mice (10 months of age, Charles River Laboratories) were subjected to a moderate closed articular fracture of the left hind limb, as previously reported [20, 21]. Eleven mice received a single, 6 μL intra-articular injection of IL-1Ra (900 μg , anakinra, Kineret[®], Swedish Orphan Biovitrum (SOBI)) in the injured knee only immediately following fracture (fx). The control group received no treatment (n=11), so that the natural response to fracture, including the presence of immune cells with the intra-articular environment could be assessed and compared to the human samples. Three mice from no treatment or IL-1Ra treatment were sacrificed 7 days post-fracture for initial assessment, and subsequently 8 mice from each group were sacrificed at 14 days post-fracture (Figure 2B). Hind limbs were scanned by microCT (VivaCT 80, Scanco, 19.5 μm resolution), followed by processing for histology. Formalin-fixed paraffin embedded knee joints were sectioned at 8 μm thickness. Sections were stained with H&E

for assessment of synovitis [21, 22], and immunohistochemistry (IHC) was used to quantify immune cells in the synovium, including macrophages, CD4 T cells, and CD8 T cells.

Mouse synovial fluid (SF) was collected at the time of sacrifice using a previously reported technique of swabbing the joint with a 2mm punch of an alginate pad [23] with modification of the digestion buffer to maintain cell viability. Briefly, each target joint was opened by suprapatellar tenotomy under magnification using a dual-head operating microscope (custom dual-view Olympus SZ61 stereomicroscopes with motorized focus; Olympus, Waltham, MA). The quadriceps tendon was transected proximal to the patella, and the patella was translated anteriorly, opening the joint space allowing the joint cavity to be swabbed with the 2mm punch (Supplement S1). For this study, the pad was dissolved in 100 μ l of PBS with 50 μ M trisodium citrate and 1mM disodium EDTA for 5 mins at room temperature followed by 5 mins at 37°C. The isolated cells were then pelleted by centrifugation at 1200 rpm at room temperature for 5 minutes and the supernatant was removed without disturbing the cell pellet. The digestion buffer was replaced with 100 μ l of RPMI + 10% FBS media. For the first pilot experiment at Day 7 post-fx, all fractured (n=3) and contralateral control (n=3) SF samples were combined for both treatment groups in an attempt to ensure adequate cell numbers (n=1 pooled SF sample per group) (Figure 2B). For the subsequent collection of samples at Day 14, sample sizes were increased (Figure 2B) with SF samples from 4 fractured limbs for both treatment groups being pooled again in an attempt to ensure adequate cell numbers (n=2 pooled SF samples per group). Prior to cell surface staining, red blood cells were lysed from all mouse synovial fluid samples using BD PharmLyse, an ammonium chloride based lysing buffer (BD; San Jose, CA).

Whole blood was collected in heparinized tubes. To isolate peripheral blood mononuclear cells (PBMCs), blood was overlaid on Ficoll, with PBMCs separated by density gradient centrifugation. After transferring the PBMCs to a new tube, the cells were washed twice with HBSS and saved for cell staining. Both synovial fluid cells and PBMCs were stained as described above using a panel of fluorescent antibodies that includes markers for innate and adaptive cell subsets, including monocytes, macrophages, dendritic cells, neutrophils, B and T cells (Figure 3B).

Using paraffin sections of knee joints, macrophages were stained using a general murine macrophage marker, F4/80. Antigen retrieval was performed using 0.01% proteinase K (Sigma-Aldrich P2308) for 5 minutes at 37°C, followed by endogenous peroxidase quenching with 3% H₂O₂ in methanol for 60 minutes. Sections were then incubated with the rat anti-mouse monoclonal antibody against a surface marker of macrophages (F4/80, Serotec MCA497G) at a 1:150 dilution (conc. 3.3 μ g/ μ l) for 1 hour at room temperature. T cells were stained with either CD4 or CD8 antibody. Antigen retrieval was performed using tris-EDTA buffer, pH 9.0 (Abcam ab93684) for CD4 and citrate buffer, pH 6.0 (Vector Labs H-3300) for CD8 at 95°C for 15 minutes, followed by endogenous peroxidase quenching with 3% H₂O₂ in methanol for 30 minutes. Sections were then incubated with a rabbit anti-mouse CD4a monoclonal antibody (Abcam ab183685) or a rabbit anti-mouse CD8a monoclonal antibody (Abcam ab209775) at a 1:100 dilution (conc. 6.95 μ g/ μ l for CD4a and 6.3 μ g/ μ l for CD8a) at 4°C overnight. Antibodies were diluted in blocking serum matched to appropriate species-specific IgG detection kits with negative controls receiving serum only.

Following incubation, appropriate polymer detection kits were utilized (for F4/80, ImmPRESS HRP goat anti-rat, mouse adsorbed IgG kit MP-7444; for CD4 and CD8 ImmPRESS HRP horse anti-rabbit IgG kit MP-7401, Vector laboratories), followed by DAB substrate (SK-4100, Vector laboratories) for chromogenic detection and hematoxylin counter stain (H-3494, Vector laboratories). Digital images of the joint tissue were obtained (BX53 with DP73 camera, cellSens software, Olympus, Center Valley, PA) for stained and negative control sections. Positive cells within four regions of the synovium (regions adjacent to the medial and lateral femoral condyles and tibial plateau) for each antibody were counted by two blinded graders for all joints, and the average cell count reported.

All statistical analyses were performed using Statistica software (TIBCO, Palo Alto, CA). Non-parametric analyses were performed to assess differences between untreated and IL-1Ra treated mice in synovitis, immune cells quantified from IHC, and whole blood immune cell subsets, with significance reported at the 95% confidence level. Wilcoxon's matched pairs test was used to compare differences between control and fractured limbs at each time point for each treatment independently. The Mann-Whitney U test was used to compare differences between treatments and between day 7 and day 14 independently.

Results:

Human Articular Fracture Synovial Fluid Samples.

In this pilot study, we tested the feasibility of immune phenotyping synovial fluid-derived cells from patients with intra-articular fracture with the potential complications of hematoma and tissue fragments within the joint. Approximately 1 ml of synovial fluid was obtained from 6 patients (2 males, 4 females) with an ankle fracture from 1 to 14 days after injury (Figure 1A). Red blood cell pellets were visible in all samples during processing and treated with lysis buffer. All samples were successfully processed for immune phenotyping and viable CD45+ counts reported (Figure 1C). As a preliminary analysis of immune cell subsets to confirm feasibility in the ankle synovial fluid, we performed flow cytometry by staining for pan-markers: CD19, CD3, and CD14, which distinguish B cells, T cells, and monocytes, respectively (Figure 1B). The percent cell subsets of each cell type are reported in Figure 1D. Gated on CD45+ cells, the majority of the cells were adaptive immune cells, dominated by CD3+ T cells ($63.68\% \pm 8.66\%$) and CD19+ B cells ($9.96\% \pm 8.78\%$) with a minimal number of CD14+ monocytes ($0.08\% \pm 0.12\%$) (Figure 1C). Within the CD3+ population, we observed both CD4 T cells ($48.90\% \pm 16.73\%$) and CD8 T cells ($35.80\% \pm 7.90\%$) (Figure 1E). This study demonstrates the feasibility of immune profiling of human ankle-derived synovial fluid and the need for an in-depth analysis of the CD4 and CD8 T cell subsets that home to the site of injury.

Mouse Articular Fracture Model.

Synovial fluid was evaluated at Day 7 and Day 14 days after articular fracture, as joints showed maximal synovitis in the synovial tissue at these time points in previous experiments [21, 24]. Additional post-injury characterization of immune cells was assessed via whole blood immune cell phenotyping and immune cell-specific IHC in synovial tissue for the mouse study.

Day 7 Synovial Fluid and Whole Blood Immune Cell Phenotyping.—Murine synovial fluid cells were successfully isolated from fractured and contralateral non-fractured control limbs at Day 7 post-fracture. Cell viability of the pooled synovial fluid samples was as follows: 99.1% for fractured limbs and 65.0% for contralateral control limbs of the untreated groups; 99.0% for fractured limbs and 82.5% for contralateral control limbs of the IL-1Ra treated group. As demonstrated by flow cytometry, CD45+ leukocytes were present in significant numbers in synovial fluid from fractured, but not control limbs (Figure 3B, Table 1). Subset analysis was not performed on contralateral control synovial fluid due to the small number of cells (Table 1). Gated on CD45+ cells (Figure 3C), immune cell frequencies in pooled synovial fluid from fractured limbs of both untreated and IL-1Ra treated mice included adaptive CD19+ B cells (untreated 34.7%, IL-1Ra 28.1%) and CD3+ T cells (untreated 13.2%, IL-1Ra 16.3%) and innate cell subsets gated on non-T cells and B cells, including of NK cells, macrophages, dendritic cells, and monocytes (Figure 3D, Supplement Table S1). At Day 7 after injury, the immune cell subsets in synovial fluid in B6 mice were similar to those in human synovial fluid, with the presence of adaptive immune cells, including T cells and B cells, and low frequencies of monocytes. Comparison of immune cell frequencies in whole blood compared to pooled synovial fluid at Day 7 are shown in Figure 3D. Macrophages showed the greatest enrichment in synovial fluid (untreated 30.6%, IL-1Ra 34.5%) compared to whole blood (untreated $6.0 \pm 2.2\%$, IL-1Ra $5.4 \pm 2.7\%$) at 7 days post-fracture. Whole blood immune cell frequencies were not significantly different between untreated and IL-1Ra treatment at Day 7 post-fracture (Figure 3D, Supplemental Table S1).

Day 14 Synovial Fluid and Whole Blood Immune Cell Phenotyping.—

Contralateral control limb synovial fluid was not analyzed via flow cytometry at Day 14 due to the findings at Day 7, in which detectable viable cells were too low to perform cell subset analysis. For fractured limbs at Day 14 post-fracture, synovial fluid samples pooled from 4 limbs (n=2 per group) of both untreated and IL-1Ra treated groups had insufficient cell counts for flow cytometric analysis (Table 1). Consequently, fourteen days after fracture the synovial fluid immune cell subsets in B6 mice could not be compared with human samples.

For whole blood immune cell phenotyping at Day 14, IL-1Ra treatment did not have a statistically significant effect on immune cell frequencies (Figure 3F, Supplemental Table S1). In comparing Day 14 to Day 7 for whole blood, both treatment groups had an increase in percentages of macrophages ($p = 0.02$) and modest increase in monocytes ($p=0.02$) from Day 7 to Day 14 (Figure 3E, 3F, Supplemental Table S1). Treatment with IL-1Ra also resulted in increases in percent cell subsets of NK cells ($p=0.01$) and dendritic cells ($p=0.01$) from Day 7 to Day 14 that was not found without treatment (Figure 3E, 3F, Supplemental Table S1).

Synovitis Histopathology.—At both Day 7 and 14 post-fx, fractured limbs had significantly greater synovitis scores compared to contralateral control limbs ($p = 0.03$). However, synovitis scores were not significantly different with IL-1Ra treatment at Day

7 post-fracture (untreated 10.0 ± 7.0 , IL-1Ra 15.7 ± 6.1 , $p=0.38$) or Day 14 post-fracture (untreated 8.3 ± 4.3 , IL-1Ra 12.2 ± 7.7 , $p=0.33$).

Immunohistochemistry.—Immune cells in the synovial tissue of control and fractured limbs were quantified via IHC (Figure 4B and Supplemental Figure S2). The quantity of F4/80+ macrophage cells was not significantly different between contralateral control and fractured limbs or between untreated and IL-1Ra at Day 7. However, at Day 14, F4/80+ macrophages in fractured limbs for groups with and without IL-1Ra were significantly elevated compared to contralateral control limbs (untreated, $p=0.01$; IL-1Ra, $p=0.017$, Figure 4C). Similar trends were observed for CD4+ T cells in the synovium, with fractured limbs showing greater numbers of positive cells compared to contralateral control limbs at Day 14 only (untreated, $p=0.06$; IL-1Ra, $p=0.06$, Figure 4D). CD8+ T cells were not significantly different between fractured and contralateral control limbs for either treatment at either time point. IL-1Ra treatment resulted in significantly lower CD8+ T cells compared to no treatment ($p=0.03$) in the contralateral control limbs at Day 14, (Figure 4E). However, there were still significantly more CD8+ T cells in both fractured and control limbs at Day 14 compared Day 7 post-fracture ($p<0.019$), suggesting a systemic change as opposed to a local effect of the injury.

Discussion:

This study describes a novel method to isolate viable cells from synovial fluid in the human and murine models following intra-articular fracture. These techniques demonstrate the feasibility of phenotyping immune cell subsets via polychromatic flow cytometry from a small volume of synovial fluid in patients and mice with closed articular fracture. While the presence of pro-inflammatory cytokines in synovial fluid after intra-articular fracture is well documented, the phenotypes of immune cells in the synovial fluid following articular fracture have not been characterized. This work describes techniques that can be used to identify immune cells that are present in synovial fluid following articular fracture.

Immune cell phenotyping in synovial fluid has been reported for inflammatory arthritis, most commonly for rheumatoid arthritis (RA) patients, and with end-stage OA in patients receiving total joint replacements. Penatti et al. compared synovial fluid samples from both RA patients and OA patients with active synovitis and reported finding different immune cell signatures, as characterized by different T cell frequencies and cytokine profiles [25]. With respect to joint injury, alterations in the balance of T cell subsets quantified in synovial fluid has also been associated with increased knee joint laxity following allograft reconstruction from ACL injury in the knee [26]. Although characterized in long bone fracture callus [27], immune cell profiling in synovial fluid following articular fracture has not been reported. Future studies will expand upon our investigation into cellular populations with the synovial fluid using high-dimensional flow cytometry and an expanded panel of markers.

A limitation of this pilot study was that cellular immune profiling of mouse synovial fluid required pooling from multiple mice. At 7 days post-fracture, 3 murine synovial fluid samples were pooled to yield sufficient cell numbers for profiling, thereby demonstrating

feasibility of this approach of utilizing pooled samples at early time point post-injury. These data are valuable for powering future studies (Supplement S3). Subsequently, we pooled samples from four animals at 14 days post-fracture but were unable to obtain a sufficient number of immune cells for phenotyping via polychromatic flow cytometry, suggesting an acute increase in synovial fluid cellularity in the injured mouse joint during the first 7 days post-fracture that was markedly reduced by 14 days post-fracture. A collagenase-induced model of OA in mice reported a return of cellularity to basal levels at 7 days based on analyses of pooled synovial fluid acquired by washout pooled from 7 animals [28]. It is interesting to note that the cell counts in the human synovial fluid samples also decreased with time since injury (Figure 1C), similar to the decrease of cells in mouse synovial fluid. Moving forward, cellular profiling will be necessary to determine the kinetics of immune cell infiltration into the synovial fluid after articular fracture.

The limited number of immune cells at 14 days following intra-articular fracture in the murine model does raise questions about the value of synovial fluid aspiration to detect immune cells involved in the response to intra-articular fracture over time. Biomarker analysis of mouse synovial fluid following fracture similarly revealed that inflammatory cytokine concentrations were greatest within 1–2 days of injury and dropped significantly by day 7 [29]. Interestingly, immunohistochemistry demonstrated a significant cellular infiltrate in the synovium including immune cells at both 7 and 14 days, in contrast to the limited number of cells present in synovial fluid at 14 days after fracture. 56 days are required for B6 mice to develop well-established PTA, while humans can develop end stage PTA in 18–24 months after intra-articular fracture [20, 30, 31]. Given this the time point of 14 days after fracture in B6 mice may be equivalent to a time point of two to three months after fracture in humans. Further work is needed to determine if these differences in immune cell subsets between synovial fluid and synovium are reproducible in mice as well as humans. In clinical situations involving acute processes such as infection or acute inflammatory arthritis, synovial fluid analysis is often very revealing [32]. With idiopathic OA, immune cell infiltration in synovial tissue has been reported [33–35]. However, there is little evidence comparing immune cell subsets in synovial fluid and synovial tissue in humans or mice for specific conditions, specifically following articular fracture. Whether synovial biopsy will ultimately be more revealing than simple synovial fluid aspiration is unknown. We were unable to establish if inhibiting IL-1 following fracture altered the immune cell phenotypes in synovial fluid immune cells at the time points evaluated, but differences were identified in CD8+ T cells in synovial tissue with IL-1Ra treatment. Future work will require a combined approach of synovial fluid, whole blood and tissue phenotyping of immune cell subsets from the acute phase to the early development of PTA.

The comparison of human and murine immune cells is limited to synovial fluid in this work. However, this limited data set offers the opportunity to compare and contrast immune cells profiles of synovial fluid from humans and mice following articular fracture to begin to characterize the immune response to injury. Further work is needed to determine immune cell subsets in whole blood in both humans and mice following intra-articular fracture to assess whether the changes in whole blood after intra-articular fracture are similar. This work suggests that this methodology for synovial fluid immune phenotyping in combination with whole blood analysis in patients with articular fractures may assist

in identifying a cellular profile that is pathogenic versus non-pathogenic and promotes healing. Future investigations using *in vivo* models could aid in unlocking the mechanisms of disease pathogenesis in patients and identifying immune factors of articular fracture that are predictive of PTA susceptibility to establish immunomodulatory therapeutic targets.

Supplementary Material

Refer to Web version on PubMed Central for supplementary material.

Acknowledgments.

We would like to acknowledge Jonas Herfarth, Carrie Williams, and Stephen Johnson for technical assistance with the animal study, histology and immunohistochemistry. This study was supported by DoD TRP W81XWH-12-1-0621, DoD TRP W81XWH-12-1-0622, and NIH NIA P30 AG028716.

References

1. Brown TD, Johnston RC, Saltzman CL, Marsh JL, Buckwalter JA. Posttraumatic osteoarthritis: a first estimate of incidence, prevalence, and burden of disease. *J Orthop Trauma* 2006; 20: 739–744. [PubMed: 17106388]
2. Punzi L, Galozzi P, Luisetto R, Favero M, Ramonda R, Oliviero F, et al. Post-traumatic arthritis: overview on pathogenic mechanisms and role of inflammation. *RMD open* 2016; 2: e000279–e000279. [PubMed: 27651925]
3. Lubbeke A, Salvo D, Stern R, Hoffmeyer P, Holzer N, Assal M. Risk factors for post-traumatic osteoarthritis of the ankle: an eighteen year follow-up study. *Int Orthop* 2012; 36: 1403–1410. [PubMed: 22249843]
4. Anderson DD, Marsh JL, Brown TD. The pathomechanical etiology of post-traumatic osteoarthritis following intraarticular fractures. *Iowa Orthop J* 2011; 31: 1–20. [PubMed: 22096414]
5. Cross JD, Ficke JR, Hsu JR, Masini BD, Wenke JC. Battlefield orthopaedic injuries cause the majority of long-term disabilities. *J Am Acad Orthop Surg* 2011; 19 Suppl 1: S1–7. [PubMed: 21304041]
6. Giannoudis PV, Tzioupis C, Papathanassopoulos A, Obakponovwe O, Roberts C. Articular step-off and risk of post-traumatic osteoarthritis. *Evidence today. Injury* 2010; 41: 986–995. [PubMed: 20728882]
7. Adams SB, Reilly RM, Huebner JL, Kraus VB, Nettles DL. Time-Dependent Effects on Synovial Fluid Composition During the Acute Phase of Human Intra-articular Ankle Fracture. *Foot Ankle Int* 2017; 38: 1055–1063. [PubMed: 28891711]
8. Adams SB, Setton LA, Bell RD, Easley ME, Huebner JL, Stabler T, et al. Inflammatory Cytokines and Matrix Metalloproteinases in the Synovial Fluid After Intra-articular Ankle Fracture. *Foot & Ankle International* 2015.
9. Catterall JB, Stabler TV, Flannery CR, Kraus VB. Changes in serum and synovial fluid biomarkers after acute injury (NCT00332254). *Arthritis Res Ther* 2010; 12: R229. [PubMed: 21194441]
10. Haller JM, McFadden M, Kubiak EN, Higgins TF. Inflammatory cytokine response following acute tibial plateau fracture. *J Bone Joint Surg Am* 2015; 97: 478–483. [PubMed: 25788304]
11. Olson SA, Furman BD, Kraus VB, Huebner JL, Guilak F. Therapeutic opportunities to prevent post-traumatic arthritis: Lessons from the natural history of arthritis after articular fracture. *J Orthop Res* 2015; 33: 1266–1277. [PubMed: 25939531]
12. Furman BD, Mangiapani DS, Zeitler E, Bailey KN, Horne PH, Huebner JL, et al. Targeting pro-inflammatory cytokines following joint injury: acute intra-articular inhibition of interleukin-1 following knee injury prevents post-traumatic arthritis. *Arthritis Res Ther* 2014; 16: R134. [PubMed: 24964765]

13. Kimmerling KA, Furman BD, Mangiapani DS, Moverman MA, Sinclair SM, Huebner JL, et al. Sustained intra-articular delivery of IL-1Ra from a thermally-responsive elastin-like polypeptide as a therapy for post-traumatic arthritis. *Eur Cell Mater* 2015; 29: 124–140. [PubMed: 25636786]
14. Firestein GS, McInnes IB. Immunopathogenesis of Rheumatoid Arthritis. *Immunity* 2017; 46: 183–196. [PubMed: 28228278]
15. Zong M, Malmström V, Lundberg IE. Anakinra effects on T cells in patients with refractory idiopathic inflammatory myopathies. *Annals of the Rheumatic Diseases* 2011; 70: A80–A81.
16. Guo Q, Wang Y, Xu D, Nossent J, Pavlos NJ, Xu J. Rheumatoid arthritis: pathological mechanisms and modern pharmacologic therapies. *Bone Research* 2018; 6: 15. [PubMed: 29736302]
17. Birnhuber A, Crnkovic S, Biasin V, Marsh LM, Odler B, Sahu-Osen A, et al. IL-1 receptor blockade skews inflammation towards Th2 in a mouse model of systemic sclerosis. *Eur Respir J* 2019; 54.
18. Kraus VB, Huebner JL, Fink C, King JB, Brown S, Vail TP, et al. Urea as a passive transport marker for arthritis biomarker studies. *Arthritis Rheum* 2002; 46: 420–427. [PubMed: 11840444]
19. Yi JS, Rosa-Bray M, Staats J, Zakrojsky P, Chan C, Russo MA, et al. Establishment of normative ranges of the healthy human immune system with comprehensive polychromatic flow cytometry profiling. *PLoS One* 2019; 14: e0225512.
20. Furman BD, Strand J, Hembree WC, Ward BD, Guilak F, Olson SA. Joint degeneration following closed intraarticular fracture in the mouse knee: a model of posttraumatic arthritis. *J Orthop Res* 2007; 25: 578–592. [PubMed: 17266145]
21. Lewis JS, Hembree WC, Furman BD, Tippets L, Cattel D, Huebner JL, et al. Acute joint pathology and synovial inflammation is associated with increased intra-articular fracture severity in the mouse knee. *Osteoarthritis Cartilage* 2011; 19: 864–873. [PubMed: 21619936]
22. Krenn V, Morawietz L, Burmester GR, Kinne RW, Mueller-Ladner U, Muller B, et al. Synovitis score: discrimination between chronic low-grade and high-grade synovitis. *Histopathology* 2006; 49: 358–364. [PubMed: 16978198]
23. Seifer DR, Furman BD, Guilak F, Olson SA, Brooks SC 3rd, Kraus VB. Novel synovial fluid recovery method allows for quantification of a marker of arthritis in mice. *Osteoarthritis Cartilage* 2008; 16: 1532–1538. [PubMed: 18538588]
24. Kimmerling KA, Furman BD, Vovos TJ, Huebner JL, Guilak F, Olson SA. Bone Morphological Changes Correlate with Reduction in PTA after Articular Fracture in the MRL/MpJ Mouse. Annual Meeting of the Orthopaedic Research Society. Las Vegas, NV2015:0332.
25. Penatti A, Facciotti F, De Matteis R, Larghi P, Paroni M, Murgo A, et al. Differences in serum and synovial CD4+ T cells and cytokine profiles to stratify patients with inflammatory osteoarthritis and rheumatoid arthritis. *Arthritis Res Ther* 2017; 19: 103. [PubMed: 28526072]
26. Yang R, Zhang Z, Song B, Wang P, Wang L, Li W, et al. Ratio of T helper to regulatory T cells in synovial fluid and postoperative joint laxity after allograft anterior cruciate ligament reconstruction. *Transplantation* 2012; 94: 1160–1166. [PubMed: 23128997]
27. Konnecke I, Serra A, El Khassawna T, Schlundt C, Schell H, Hauser A, et al. T and B cells participate in bone repair by infiltrating the fracture callus in a two-wave fashion. *Bone* 2014; 64: 155–165. [PubMed: 24721700]
28. Benigni G, Dimitrova P, Antonangeli F, Sanseviero E, Milanova V, Blom A, et al. CXCR3/CXCL10 Axis Regulates Neutrophil-NK Cell Cross-Talk Determining the Severity of Experimental Osteoarthritis. *J Immunol* 2017; 198: 2115–2124. [PubMed: 28108560]
29. Lewis JS Jr., Furman BD, Zeitler E, Huebner JL, Kraus VB, Guilak, et al. Genetic and cellular evidence of decreased inflammation associated with reduced incidence of posttraumatic arthritis in MRL/MpJ mice. *Arthritis Rheum* 2013; 65: 660–670. [PubMed: 23203659]
30. Dirschl DR, Marsh JL, Buckwalter JA, Gelberman R, Olson SA, Brown TD, et al. Articular fractures. *J Am Acad Orthop Surg* 2004; 12: 416–423. [PubMed: 15615507]
31. Rivera JC, Wenke JC, Buckwalter JA, Ficke JR, Johnson AE. Posttraumatic osteoarthritis caused by battlefield injuries: the primary source of disability in warriors. *J Am Acad Orthop Surg* 2012; 20 Suppl 1: S64–69. [PubMed: 22865140]

32. Ghanem E, Parvizi J, Burnett RS, Sharkey PF, Keshavarzi N, Aggarwal A, et al. Cell count and differential of aspirated fluid in the diagnosis of infection at the site of total knee arthroplasty. *J Bone Joint Surg Am* 2008; 90: 1637–1643. [PubMed: 18676892]
33. de Lange-Brokaar BJ, Ioan-Facsinay A, van Osch GJ, Zuurmond AM, Schoones J, Toes RE, et al. Synovial inflammation, immune cells and their cytokines in osteoarthritis: a review. *Osteoarthritis Cartilage* 2012; 20: 1484–1499. [PubMed: 22960092]
34. Huss RS, Huddleston JI, Goodman SB, Butcher EC, Zabel BA. Synovial tissue-infiltrating natural killer cells in osteoarthritis and periprosthetic inflammation. *Arthritis Rheum* 2010; 62: 3799–3805. [PubMed: 20848566]
35. Hussein MR, Fathi NA, El-Din AM, Hassan HI, Abdullah F, Al-Hakeem E, et al. Alterations of the CD4(+), CD8 (+) T cell subsets, interleukins-1beta, IL-10, IL-17, tumor necrosis factor-alpha and soluble intercellular adhesion molecule-1 in rheumatoid arthritis and osteoarthritis: preliminary observations. *Pathol Oncol Res* 2008; 14: 321–328. [PubMed: 18392953]

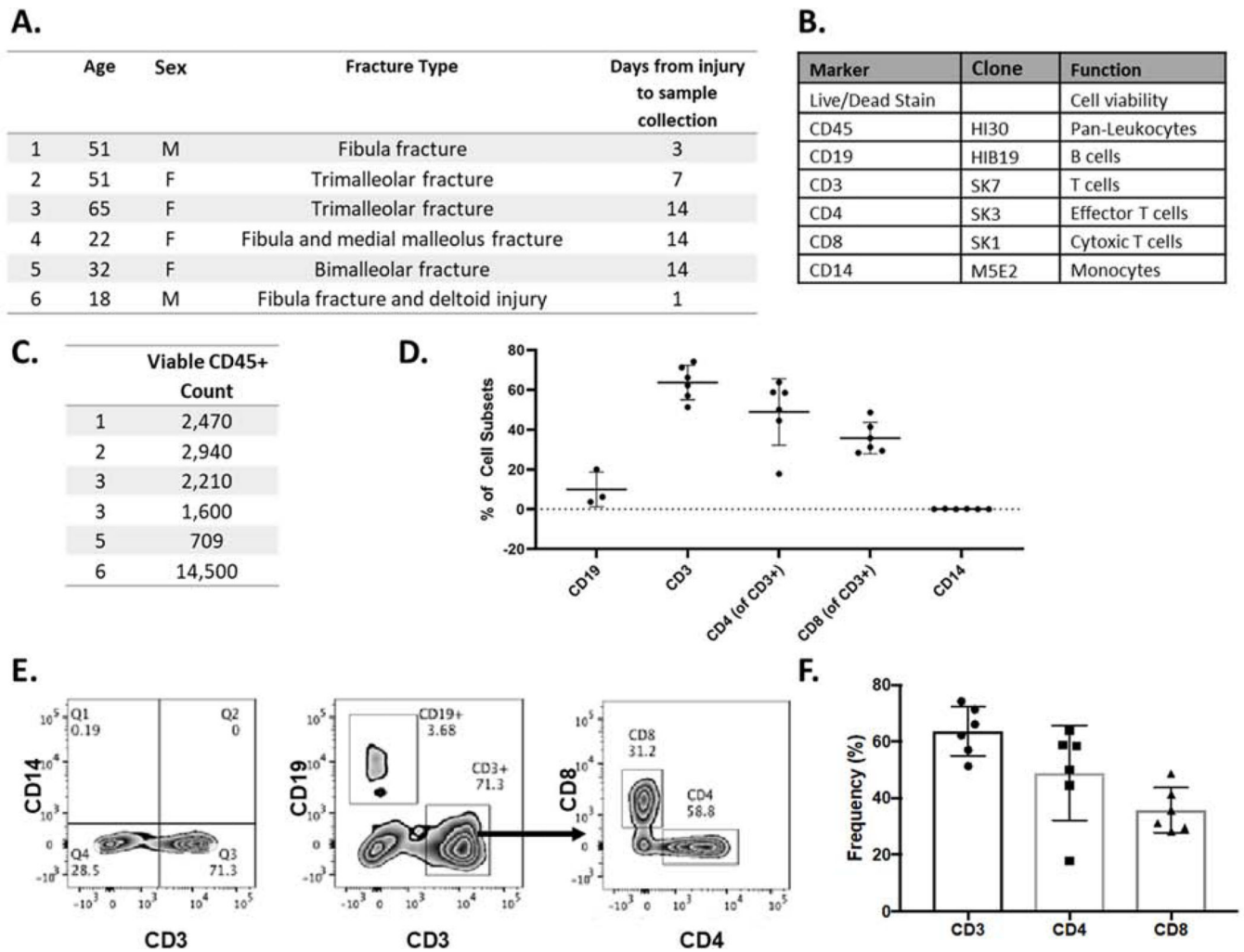
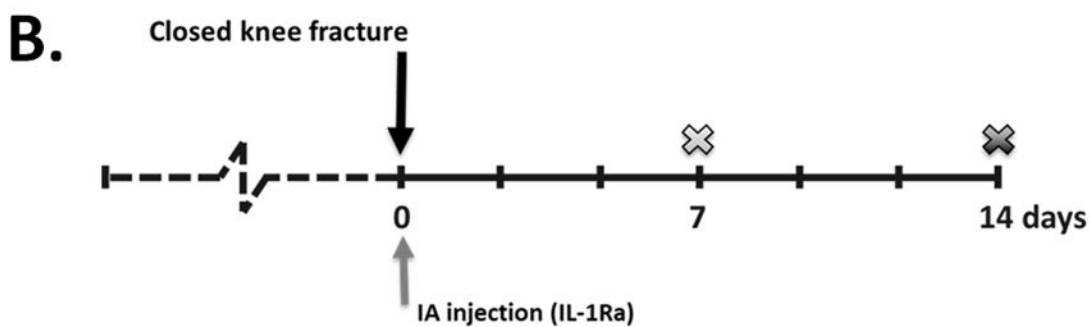
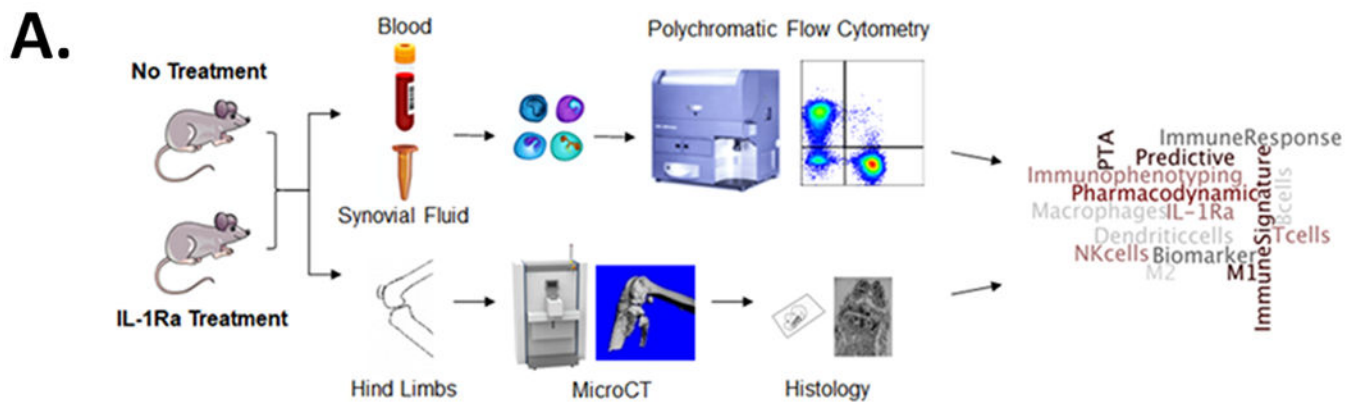


Figure 1.

Immune cells in human ankle-derived synovial fluid following articular fracture. **A)** Patient demographics for synovial fluid samples (n=6). **B)** Panel of antibodies for immune cell phenotyping in human synovial fluid. **C)** Viable CD45+ count in each sample. **D)** Percent cell subsets of immune cells for all human synovial fluid samples (mean \pm st dev). **E)** Flow cytometry analysis of a representative patient to identify B cells, T cells, and monocytes. Gated CD45+ T cells are shown in the first two plots and the CD4/CD8 T cell plot is derived from CD3 T cells. **F)** Composite data from individual patients showing the frequency of CD3 T cells (gated on CD45+ cells) and CD4 and CD8 T cells (gated on CD3 T cells). T cells constitute the majority of immune cells in human ankle-derived synovial fluid.



✕ **7 days post-fracture: No treatment (n=3); IL-Ra treatment (n=3)**

✕ **14 days post-fracture: No treatment (n=8); IL-Ra treatment (n=8)**

Figure 2.

Experimental Design. **(A)** Schematic of experimental design. **(B)** Timeline of experiments. Mice received no treatment following closed articular fracture of the knee or a single intra-articular (IA) injection of IL-1Ra immediately following fracture. At 7 days post-fracture, synovial fluid (SF) collected and pooled from 3 fractured and 3 control limbs per group, and whole blood (WB) collected for n=3 per group. At 14 days post-fracture, synovial fluid collected and pooled from 4 fractured limbs for n=2 per group, and whole blood (WB) collected for n=8 per group. Hind limbs collected from all mice for microCT and histology.

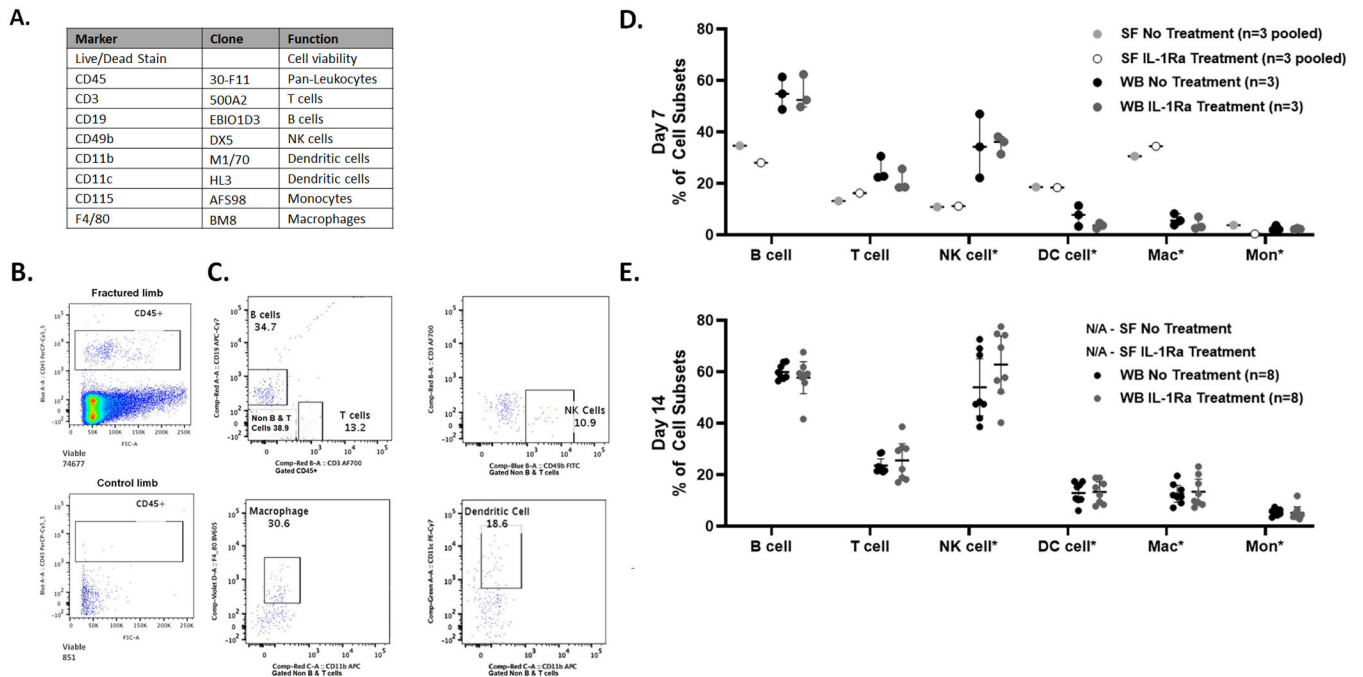
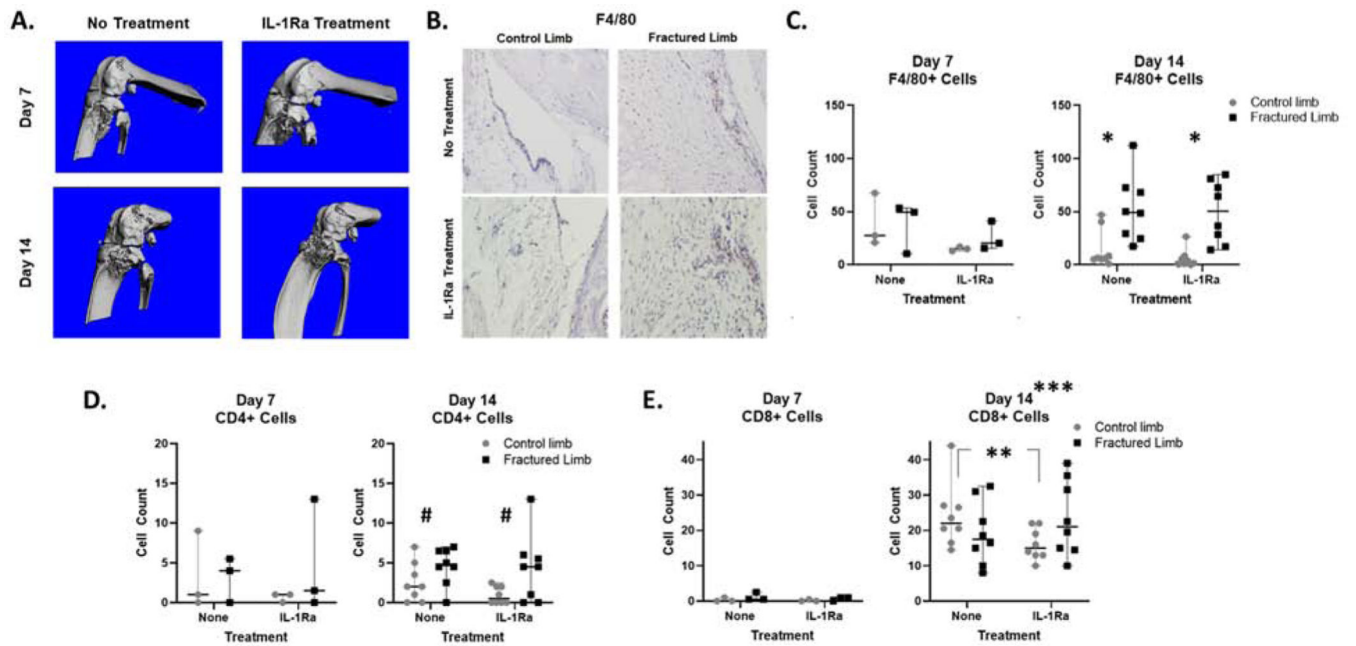


Figure 3. Immune cell phenotyping in synovial fluid and whole blood from mouse model of closed articular fracture via polychromatic flow cytometry **A)** Panel of antibodies for immune cell phenotyping. **B)** Comparison of CD45+ leukocytes in pooled synovial fluid from 3 joints at 7 days post-fracture of fractured (74,677 events) and control (851 events) limbs with no treatment. **C)** Representative example of detection of B cells, T cells, NK cells, macrophages and dendritic cells (DC) in the synovial fluid from untreated fractured limbs, gated on CD45+ for T cells and B cells and *Non-B and T cells for remaining cell subsets. **D)** Immune cell subsets at Day 7 post-fracture in synovial fluid (SF) and whole blood (WB) for both no treatment and IL-1Ra treatment (mean \pm 95% CI). **E)** Immune cell subsets at Day 14 post-fracture in whole blood (mean \pm 95% CI). Synovial fluid data Not Available (N/A) from pooled synovial fluid from 4 joints (n=2 per group) as cell count, determined by detectable events, was too low for subset analysis.

**Figure 4.**

Closed articular fracture in the mouse knee and quantification of immune cells in mouse synovial tissue following fracture. **A)** MicroCT images of fractured knee joints for both no treatment and IL-1Ra treatment at Day 7 and Day 14 post-fracture. **B)** Representative images of positive IHC staining in synovium at Day 14 in contralateral control and fractured limbs (brown=F4/80+ stain, blue=hematoxylin counter stain). **C)** Quantification of macrophages via F4/80+ cells in synovial tissue via IHC staining (Day 14, control vs fractured limb * $p = 0.017$). **D)** Quantification of CD4+ T cells in synovial tissue via IHC staining (Day 14, control vs fractured limb # $p = 0.063$). **E)** Quantification of CD8+ T cells in synovial tissue via IHC staining (Day 14 control limb, no treatment vs IL-1Ra ** $p = 0.031$; for both limbs in both groups, Day 14 vs Day 7 *** $p = 0.019$).

Table 1.
Samples collected for immune cell phenotyping in mouse knee-derived synovial fluid (SF)
following articular fracture.

Comparison of detectable events in pooled synovial fluid with and without intra-articular IL-1Ra treatment (Tx); --- indicates sample not analyzed, as previous cell count, as determined by detectable events, was too low for subset analysis.

Group	Time post-fx (days)	SF (n)	Pooled SF NonFx Limb detectable events	Pooled SF Fx Limb detectable events
No Tx No Tx No Tx	7 7 7	n=1 (3 pooled)	851	74,677
IL-1Ra IL-1Ra IL-1Ra	7 7 7	n=1 (3 pooled)	2,001	84,118
No Tx No Tx No Tx No Tx	14 14 14 14	n=2 (4 pooled per sample)	---	43
No Tx No Tx No Tx No Tx	14 14 14 14		---	247
IL-1Ra IL-1Ra IL-1Ra IL-1Ra	14 14 14 14	n=2 (4 pooled per sample)	---	117
IL-1Ra IL-1Ra IL-1Ra IL-1Ra	14 14 14 14		---	494